Non-Singular Resonance of Equatorial Waves Under the Radiation Condition[1]

YOSHIKAZU HAYASHI

Geophysical Fluid Dynamics Program,[2] Princeton University, Princeton, N. J. 08540

(Manuscript received 7 July 1975, in revised form 13 October 1975)

ABSTRACT

A response of large-scale equatorial waves to a thermal or a lateral forcing confined in the troposphere is examined analytically by imposing the radiation condition based on an equatorial beta-plane model without wind shear.

A resonant response with large finite amplitude occurs under the radiation condition, when the vertical scale of the wave coincides with that of the forcing. This "non-singular resonance" is associated with a sharp spectral peak for equatorial waves which are characterized by a small variation of the frequency with the vertical wavenumber. However, such resonant equatorial waves are not realistic, since their vertical velocity is not in phase with the imposed convective heating and their pressure is not in geostrophic balance with the meridional wind of the imposed mid-latitude disturbances.

This study suggests that the forcing cannot be imposed arbitrarily regardless of its feedback. It assures on the other hand that the equatorial waves simulated by a general circulation model are not spurious resonant waves resulting from an artificial reflection at the top of a finite-difference model.

1. Introduction

It is well known that some tropical disturbances are characterized by distinct scale and periodicities. Among them are westward-moving mixed Rossby-gravity waves (Yanai and Maruyama, 1966) of wavenumbers 3–4 and periods of 4–5 days and eastward-moving Kelvin waves (Wallace and Kousky, 1968) of wavenumbers 1–2 and periods 10–20 days.

It was pointed out by Maruyama (1967), Lindzen and Matsuno (1968) and Holton and Lindzen (1968) that these waves are consistent with the dispersion relation and structure of equatorial normal modes studied by Rosenthal (1965), Matsuno (1966) and Longuet-Higgins (1968). However, in their studies no explanation was given as to how these waves are generated and selected among the many possible equatorial normal modes.

There have been several theoretical studies to explain the selection of planetary-scale equatorial waves. The first approach was a theory of resonance to mid-latitude forcing (Mak, 1969). According to this study, the tropical atmosphere has a resonant period of 5 days and the equatorial waves derive their energy from mid-latitude disturbances. His result was also consistent with theories of wave propagation (Charney, 1969; Bennett and Young, 1971) that waves with phase speeds more westward than the mean flow may propagate into the tropics. However, Manabe *et al.* (1970) demonstrated by their GFDL general circulation model that latent heat release within the tropics is more important than the energy flux from mid-latitudes to maintain tropical disturbances.

The second approach was an instability (CISK) theory of large-scale waves coupled with cumulus convection. It was assumed that the cumulus heating is proportional to the low-level convergence. Yamasaki (1969) found, based on two-dimensional quasi-geostrophic equations, that instability occurs for large-scale waves which resemble the observed Yanai-Maruyama waves in their vertical structure. Hayashi (1970, 1971a,b) re-examined this unstable mode by using a three-dimensional primitive equation model on an equatorial beta-plane so that equatorial waves may be treated. He found that mixed Rossby-gravity waves with wavenumber 4 and period of 4 days become unstable. However, the unstable mixed Rossby-gravity waves do not attain their maximum growth rate at the observed scale, and high-frequency gravity waves are the most unstable. One way to overcome this difficulty is to assume that the cumulus heating becomes inefficient for high-frequency waves (Hayashi, 1971c). Recently Kuo (1975) has made a detailed study of this possibility.

The third explanation was the filtering effect of the atmosphere on the vertical propagation of waves. Holton (1972, 1973) showed that among various wave modes excited by localized thermal forcing, Kelvin

[1] Presented at the Ninth Conference on Hurricanes and Tropical Meteorology, 27–30 May 1975, Key Biscayne, Miami, Fla.

[2] Support provided through Geophysical Fluid Dynamics Laboratory/NOAA Grant 04-3-022-33.

waves with wavenumbers 1–2 and periods of 10–20 days are selected in the stratosphere with a certain vertical shear. However, this theory did not account for the preferred period of 4 days for mixed Rossby-gravity waves.

The fourth approach was a space-time spectral analysis of a general circulation model. Hayashi (1973, 1974) found that both mixed Rossby-gravity waves and Kelvin waves were present in a GFDL general circulation model with moist convective adjustment. These waves agree with observed waves in their period, scale, and three-dimensional structure. The convective heating localized in the western Pacific is associated with more westward phase velocity than eastward phase velocity in agreement with the space-time spectral analysis of cloud brightness data (Gruber, 1974) and the CISK theory (Hayashi, 1970). However, the spectral peak of the heating is not sharp enough to directly account for the distinct periodicity of mixed Rossby-gravity waves in the stratosphere by the CISK theory alone. One might argue that these waves are spurious resonant waves resulting from an artifical reflection at the top of a finite-difference model as had been warned by Lindzen *et al.* (1968).

The same criticism may also apply to the two-layer finite-difference model used by Mak (1969) for studying the resonance associated with lateral forcing. A resonance also occurs in barotropic models of Matsuno (1966) and Bennett and Young (1971) since there is no vertical propagation of energy. Recently, Lamb (1973) re-examined the response of equatorial waves to mid-latitude forcing by a model in which the wave energy is allowed to leak from the troposphere. She found that a quasi-resonance is still possible in her model and further showed that the upward flux of energy due to the resonant wave can be enhanced by the convective heating associated with the wave. Instead of imposing a radiation condition rigorously on her analytical model, she assumed without justification that the vertical structure of the forced wave is everywhere the same as that of the tropospheric forcing characterized by a complex vertical wavenumber which gives a net upward flux of energy. However, it is not clear whether the wave energy leaking from the troposphere into the stratosphere is further reflected from above, since her analytical solution, which amplifies indefinitely with height, is not valid above the troposphere.

In studying the resonance of equatorial waves one must be very careful of a spurious reflection from the top, since equatorial waves are not reflected by the stratification or zonal flow, if their vertical scale is small (Lindzen, 1967). In comparing resonant waves with observed waves one must examine not only the wavenumber-frequency response but also the structure peculiar to resonant waves.

In the present paper we shall re-examine the resonance of equatorial waves by imposing the radiation condition that no wave energy may be reflected from infinite height. We shall first study the case of thermal forcing in Section 3 and then mid-latitude forcing in Section 4.

2. Basic equations[3]

The basic state is taken as a hydrostatic, isothermal atmosphere without basic flow as given by

$$\frac{dp_0}{dz}=-\rho_0 g, \tag{2.1}$$

$$p_0=\rho_0 RT_0=\rho_0 gH, \tag{2.2}$$

$$\rho_0(z)=\rho_0(0)e^{-z/H}. \tag{2.3}$$

The perturbation equations on an equatorial beta plane ($f=\beta y$) consist of the equations of motions, and the hydrostatic, continuity and thermodynamic equations as

$$\frac{\partial u'}{\partial t}-fv'=-\frac{1}{\rho_0}\frac{\partial p'}{\partial x}, \tag{2.4}$$

$$\frac{\partial v'}{\partial t}+fu'=-\frac{1}{\rho_0}\frac{\partial p'}{\partial y}, \tag{2.5}$$

$$\frac{\partial p'}{\partial z}=-g\rho', \tag{2.6}$$

$$\frac{\partial \rho'}{\partial t}+\nabla\cdot\rho_0\mathbf{V}'+\frac{\partial}{\partial z}\rho_0 w'=0, \tag{2.7}$$

$$\frac{\partial s'}{\partial t}+w'\frac{ds_0}{dz}=\frac{C_v}{p_0}(\gamma-1)J', \tag{2.8}$$

where

$$s\equiv C_p\ln\theta=C_v\ln p-C_p\ln\rho, \tag{2.9}$$

$$\frac{ds_0}{dz}=\frac{\kappa C_p}{H}, \tag{2.10}$$

$$s'=C_v\frac{p'}{p_0}-C_p\frac{\rho'}{\rho_0}. \tag{2.11}$$

Transforming the dependent variables as

$$\left.\begin{aligned}(u,v,w,J)&=\rho_0^{\frac{1}{2}}(u',v',w',J')\\(p,\rho)&=\rho_0^{-\frac{1}{2}}(p',\rho')\end{aligned}\right\} \tag{2.12}$$

and assuming the time and longitude dependence of the form $e^{i(\omega t+kx)}$, the perturbation equations are rewritten as

$$i\omega u-fv=-ikp, \tag{2.13}$$

[3] Symbols are defined in an appendix.

$$i\omega v+fu=-\frac{\partial p}{\partial y}, \tag{2.14}$$

$$\left(\frac{\partial}{\partial z}-\frac{1}{2H}\right)p=-\rho g, \tag{2.15}$$

$$i\omega\rho+iku+\frac{\partial v}{\partial y}+\left(\frac{\partial}{\partial z}-\frac{1}{2H}\right)w=0, \tag{2.16}$$

$$i\omega\left(\frac{1}{\gamma gH}p-\rho\right)+\frac{\kappa}{H}w=\frac{\kappa}{gH}J. \tag{2.17}$$

3. Thermal forcing

a. Gravity wave model

In order to simplify our discussion, we shall begin with internal gravity waves without a Coriolis force, since the presence of the Coriolis force does not alter our conclusions except for the dispersion relation. This problem will later be re-examined by an equatorial beta plane model.

Letting $f=0$ and neglecting the y dependence, Eqs. (2.13)–(2.17) are reduced to

$$\frac{\partial^2 w}{\partial z^2}+m^2w=\frac{\kappa}{gH}\left(\frac{\partial}{\partial z}+\frac{1}{h}-\frac{1}{2H}\right)J, \tag{3.1}$$

$$\left(\frac{\partial}{\partial z}+\frac{1}{h}-\frac{1}{2H}\right)p=\frac{g}{i\omega}\left(\frac{\partial}{\partial z}-\frac{1}{2H}\right)w, \tag{3.2}$$

where h is the so-called equivalent depth. The dispersion relation is given by

$$(gh)^{\frac{1}{2}}=\pm\frac{\omega}{k}, \tag{3.3}$$

when h is related to m as

$$m^2=\frac{\kappa}{Hh}-\frac{1}{4H^2}. \tag{3.4}$$

We shall be interested in internal gravity waves with small vertical scale such that

$$\frac{1}{H}<\frac{\partial}{\partial z}<\frac{1}{h}. \tag{3.5}$$

Then (3.1) and (3.2) are approximated as

$$\frac{\partial^2 w}{\partial z^2}+m^2w\approx\frac{\kappa}{gHh}J, \tag{3.6}$$

$$p\approx\frac{gh}{i\omega}\frac{\partial w}{\partial z}. \tag{3.7}$$

The heating is assumed to attain its maximum at $z=z_1/2$ and to vanish above the cloud top $z=z_1=10$ km, as

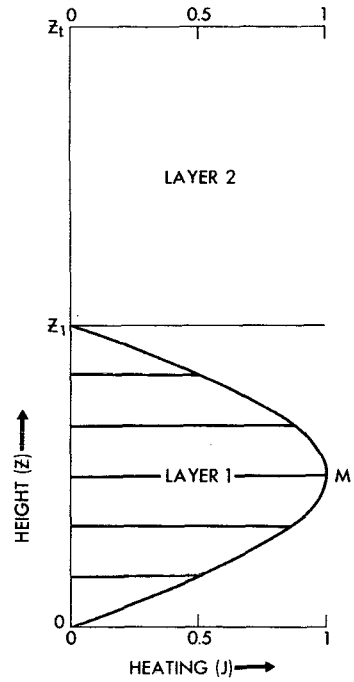

FIG. 1. Vertical profile of heating function in analytical two-layer model.

$$J=\begin{cases}J_M\sin(Mz)e^{i(\omega t+kx)}, & \text{for } 0\leqslant z\leqslant z_1\\ 0, & \text{for } z>z_1\end{cases} \tag{3.8}$$

where

$$M=\pi/z_1. \tag{3.9}$$

The vertical profile of this heating function (Fig. 1) is similar to that of the diabatic heating in the GFDL general circulation model (see Fig. 11). This problem will later be re-examined numerically using a realistic vertical profile. It is also assumed that the heating is white noise, i.e., J_M does not depend on ω and k.

1) SOLUTION BY VERTICAL MATCHING

We shall solve (3.6) by matching the solution in the adiabatic upper layer with that in the lower layer associated with a thermal forcing as illustrated in Fig. 1. This method is suited for imposing the radiation condition (Wilkes, 1949; Sommerfeld, 1949) explicitly as an upper boundary condition.

In the upper adiabatic layer, the solution consists of homogeneous solutions with upward and downward propagation of energy as

$$w^2(z)=-\frac{\kappa}{gHh}\frac{R_m^2e^{im(z-z_1)}-R_{-m}^2e^{-im(z-z_1)}}{m^2-M^2}, \tag{3.10}$$

where the complex coefficients R_m^2 and R_{-m}^2 are to be determined by the boundary conditions.

In the lower layer, the solution consists of both the homogeneous and the inhomogeneous solutions as

$$w^1(z)=-\frac{\kappa}{gHh}\frac{R_m^1\sin mz-J_M\sin Mz}{m^2-M^2}. \tag{3.11}$$

This lower layer solution satisfies the bottom boundary condition

$$w^1(0)=0. \tag{3.12}$$

The interfacial condition is

$$\left.\begin{aligned} w^1(z_1)&=w^2(z_1)\\ p^1(z_1)&=p^2(z_1)\end{aligned}\right\}. \tag{3.13}$$

The upper boundary condition is either the lid condition as

$$w(z)=0 \quad \text{at } z=z_t, \tag{3.14}$$

or the radiation condition which excludes the wave component with downward propagation of energy as

$$R_{-m}^2=0, \tag{3.15}$$

where the sign of m is determined in (3.4) in such a way that $\omega m>0$, so that R_{-m}^2 always represents downward group velocity which will be given by (3.45).

The above boundary conditions give linear algebraic equations for determining R_m as

$$\mathbf{A}_m\hat{\mathbf{R}}_m=\mathbf{A}_M\hat{\mathbf{J}}_M, \tag{3.16}$$

where

$$\hat{\mathbf{R}}_m\equiv\begin{pmatrix}R_m^2\\ R_m^1\end{pmatrix}, \quad \hat{\mathbf{J}}_M\equiv\begin{pmatrix}0\\ J_M\end{pmatrix}. \tag{3.17}$$

In case of the radiation condition, the above matrices are

$$\mathbf{A}_m=\begin{pmatrix}1, & -\sin mz_1\\ im, & -m\cos mz_1\end{pmatrix}, \tag{3.18}$$

$$\mathbf{A}_M=[\mathbf{A}_m]_{m=M}. \tag{3.19}$$

It should be noted that the denominators of the solutions (3.10) and (3.11) vanish as $m=\pm M$. However, in case of the radiation condition no singularity occurs, since the numerator also goes to zero. In the following we shall prove this for $m=+M$. It may similarly be proven for $m=-M$.

In case of the radiation condition the determinant does not vanish.

$$|\mathbf{A}_m|=-me^{-imz_1}\neq 0. \tag{3.20}$$

This assures that (3.16) has a solution of the form

$$\hat{\mathbf{R}}_m=\mathbf{A}_m^{-1}\mathbf{A}_M\hat{\mathbf{J}}_M. \tag{3.21}$$

The explicit form of R_m is

$$\left.\begin{aligned} R_m^1&=J_M\frac{M\cos Mz_1-im\sin Mz}{me^{-imz_1}}\\ R_m^2&=J_M\frac{M\cos Mz_1\sin mz_1-m\cos mz_1\sin Mz_1}{me^{-imz_1}}\end{aligned}\right\}. \tag{3.22}$$

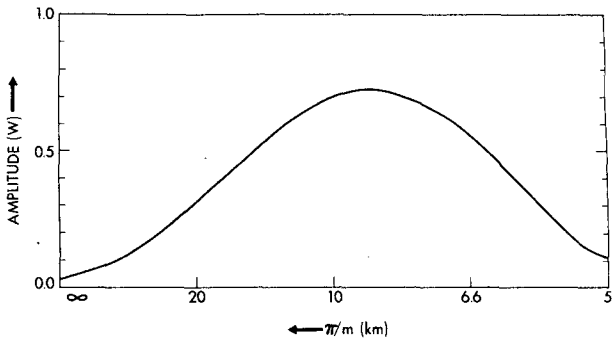

FIG. 2. Amplitude of w at $z=7.5$ km as a function of m under the radiation condition.

As m approaches M, we have

$$\lim_{m\to M}\hat{\mathbf{R}}_m=\hat{\mathbf{J}}_M. \tag{3.23}$$

Thus the solutions (3.10) and (3.11) become indeterminate as

$$\lim_{m\to M}w(z)=\frac{0}{0}. \tag{3.24}$$

Differentiating the numerator and the denominator of (3.10) and (3.11) by m and putting $m=M=\pi/z_1$ (L'Hôpital's rule), the resonant solution[4] is given explicitly by

$$\left.\begin{aligned} \lim_{m\to M}w^1(z)&=\frac{\kappa}{gHh}J_M\frac{(-i+1/\pi)z_1\sin Mz-z\cos Mz}{2\pi/z_1}\\ \lim_{m\to M}w^2(z)&=\frac{\kappa}{gHh}J_M\frac{z_1e^{iM(z-z_1)}}{2\pi/z_1}\end{aligned}\right\}. \tag{3.25}$$

This resonant solution attains its maximum a little above the level of maximum heating ($z=z_1/2$). Fig. 2 shows the amplitude of w as a function of m, illustrating that the amplitude attains its maximum near $m=M$ under the radiation condition. In other words a resonant response with a large finite amplitude occurs under the radiation condition when the vertical scale (π/m) of the wave in a free isothermal atmosphere coincides with the vertical scale (π/M) of the forcing.

Let us next examine the case of a lid condition. The matrices and the determinant of (3.16) are

$$\mathbf{A}_m=\begin{pmatrix}-\sin m(z_t-z_1), & -\sin mz_1\\ m\cos m(z_t-z_1), & -m\cos mz_1\end{pmatrix}, \tag{3.26}$$

$$\mathbf{A}_M=[\mathbf{A}_m]_{m=M}, \tag{3.27}$$

$$|\mathbf{A}_m|=m\sin mz_t. \tag{3.28}$$

[4] Alternatively, this resonant solution may be obtained directly from (3.1) with $m=M$ by assuming the solution of the form $(Az+B)e^{\pm iMz}$.

This determinant vanishes if

$$m=M_q\equiv\frac{q\pi}{z_t},\quad q=1,2,3\ldots. \tag{3.29}$$

The explicit form of R_m^1 under the lid condition is given by

$$R_m^1=J_M\frac{M\sin m(z_t-z_1)\cos Mz_1+m\cos m(z_t-z_1)\sin Mz_1}{m\sin mz_t}. \tag{3.30}$$

If $m=M_q$, the denominator of (3.30) vanishes and R_m^1 becomes infinite provided that $M_q\neq M$. If $m=M_q=M$, both the denominator and the numerator of (3.30) vanish. Applying L'Hôpital's rule we have

$$\lim_{m\to M}R_m^1=\frac{0}{0}=\left(\frac{\sin 2Mz_1}{2M}+z_t-z_1\right)J_M\neq J_M. \tag{3.31}$$

Therefore from (3.11), we find

$$\lim_{m\to M}w^1(z)=\frac{(0/0)-1}{0}=\infty. \tag{3.32}$$

Thus we confirm that resonance associated with infinite amplitude occurs under a lid, when a multiple of the vertical scale (π/m) of the wave coincides with the height (z_t) of the lid.

If this problem is solved as an initial value problem, the amplitude increases indefinitely with time[5] under the lid condition in the absence of dissipation, while the amplitude will increase toward some large finite value under the radiation condition. Hereafter the resonance associated with infinitly large amplitude will be called "singular resonance," while the resonance associated with large finite amplitude under the radiation condition will be called "non-singular resonance."

It is well known that in the presence of dissipation the radiation condition is simulated by raising the lid to infinite height, since the wave decays with height before being reflected by the lid. This fact is proven as follows.

Putting $w=0$ at $z=z_t$ in (3.10), we have

$$R_{-m}^2/R_m^2=e^{2im(z_t-z_1)}. \tag{3.33}$$

Now in the presence of Newtonian cooling or Rayleigh friction, m becomes complex $(m=m_r+im_i)$ and the reflection coefficient is given by

$$R_{ef}\equiv|R_{-m}^2/R_m^2|=e^{-2m_i(z_t-z_1)}<1. \tag{3.34}$$

Therefore the amplitude of the reflected wave (R_{-m}^2) becomes much smaller than that of the incident wave (R_m^2), if the lid (z_t) is raised sufficiently high.

It will be of interest to examine how the resonance under a lid condition in the presence of dissipation approaches the non-singular resonance under the radiation condition as the lid is raised higher. For this purpose it is simpler to solve the same problem by a method of vertical normal mode expansion as will be shown below. This method is also convenient in solving the problem of resonance of equatorial waves to lateral forcing under the radiation condition in Section 4.

2) Solution by vertical expansion

We shall solve the same equation [(3.6)] by expanding the following vertical profile of the heating,

$$J=\begin{cases}J_0\sin M_0z, & \text{for } 0\leqslant z\leqslant z_1\\ 0, & \text{for } z>z_1\end{cases}, \tag{3.35}$$

in terms of the vertical normal modes under a lid as

$$J=\sum_{q=1}^{\infty}J_q\sin M_qz, \tag{3.36}$$

where

$$M_0=\pi q_0/z_1, \tag{3.37}$$

$$M_q=\pi q/z_t,\ q=1,2,3\ldots. \tag{3.38}$$

The projection coefficient is given by

$$J_q=J_0\frac{2\delta q_0}{\delta q+q_0}\frac{\sin\pi(\delta q-q_0)}{\pi(\delta q-q_0)}, \tag{3.39}$$

where

$$\delta=z_1/z_t. \tag{3.40}$$

In determining J_q the following integrals have been

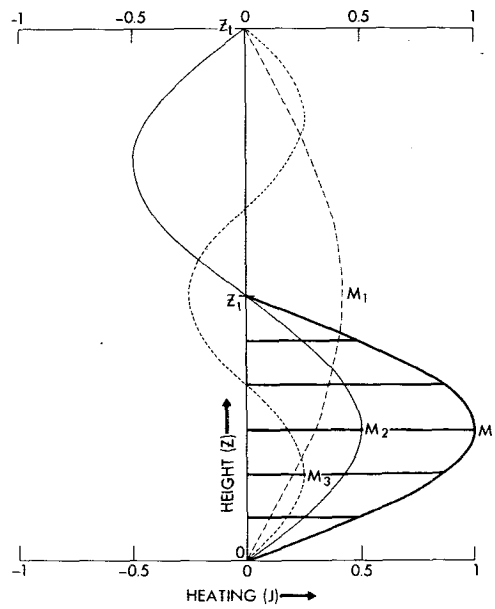

FIG. 3. Projection of vertical profile of heating (M) into vertical normal modes (M_q) under a lid $(z=z_t)$.

[5] The time dependence is of the form $te^{i\omega t}$. For a general resonant solution in a closed domain, see Orlanski (1972).

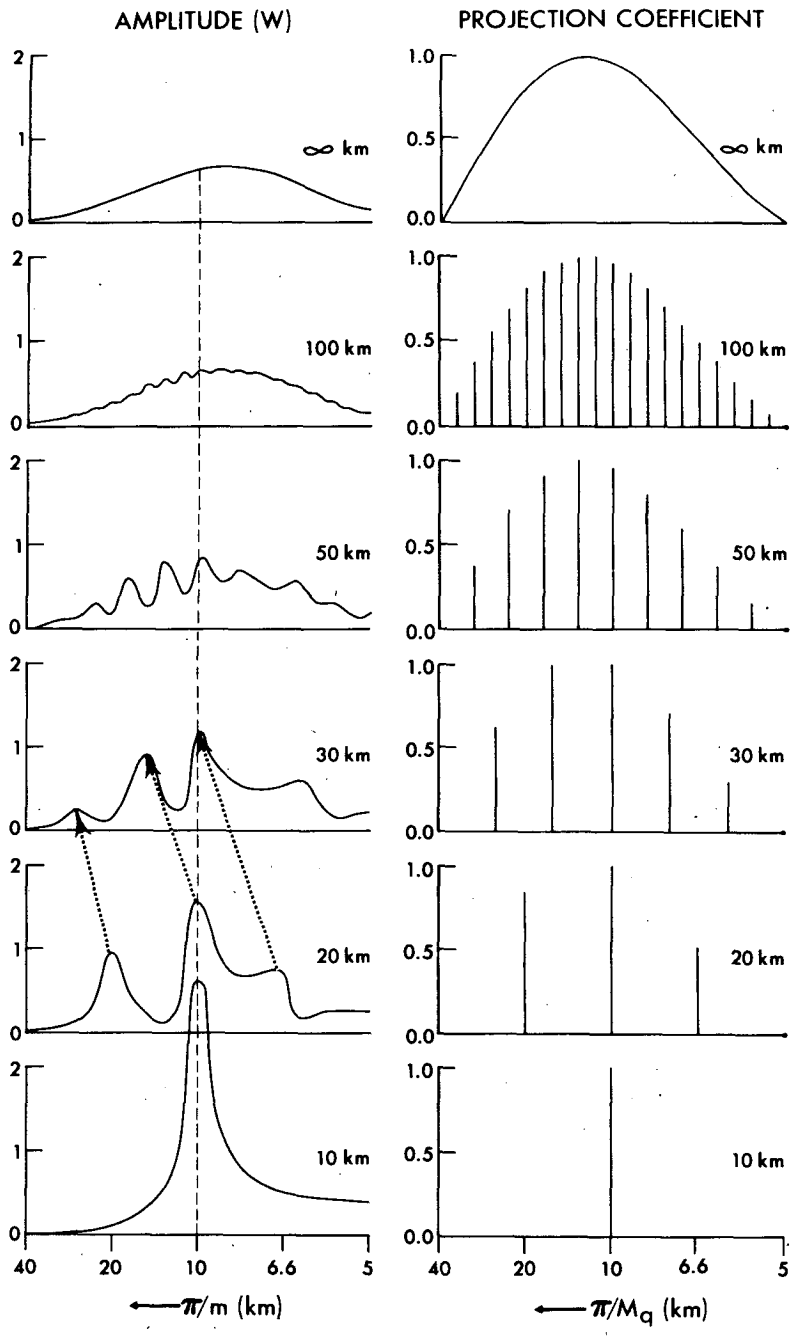

FIG. 4. Amplitude of w at $z=7.5$ km as a function of m for various heights ($z_t=10-\infty$ km) of lid [left] and absolute value of projection coefficient (normalized by its maximum) as a function of M_q of vertical normal mode for various heights of lid [right].

used:

$$\int_0^{z_1} \sin\left(q_0\pi\frac{z}{z_1}\right)\sin\left(q'\pi\frac{z}{z_t}\right)dz=z_t\frac{\delta q_0}{q_0+\delta q'}\frac{\sin\pi(q_0-\delta q')}{\pi(q_0-\delta q')} \tag{3.41}$$

$$\int_0^{z_t} \sin\left(q\pi\frac{z}{z_t}\right)\sin\left(q'\pi\frac{z}{z_t}\right)dz=\frac{z_t}{2}\frac{\sin\pi(q-q')}{\pi(q-q')}. \tag{3.42}$$

Fig. 3 illustrates how the heating confined in the lower layer is projected into various vertical normal modes.

The solution of (3.6) is readily given as

$$w(z)=\frac{\kappa}{gHh}\sum_{q=1}^{\infty}\frac{J_q\sin M_q z}{m^2-M_q^2}. \tag{3.43}$$

This solution shows explicitly that singular resonance

occurs under the lid condition, if m coincides with M_q of the vertical normal modes. In order to remove the singularity at $m=M_q$ in (3.43), we shall add to m a small imaginary part which may physically be interpreted as the effect of Newtonian cooling or Rayleigh friction. It is noted that (3.43) has a vertical variation of phase, since m is complex, although a single vertical mode with real M_q does not tilt.

Fig. 4 shows that resonant peaks occur at $m=M_q$ and that a maximum response occurs for the vertical normal mode which is associated with the vertical scale of the forcing ($M_q=M$) and hence the largest projection coefficient (J_q). The higher the lid is raised, the more vertical modes and hence more resonant peaks emerge, until the envelope curve of the numerous resonant peaks coincides with the response curve (Fig. 2) given by the explicit radiation condition.

Fig. 4 may give the impression that the resonant peak occurs at $\pi/m=10$ km at whatever level the lid is placed. This is merely because the lid is placed at a multiple of the vertical scale (z_1) of the forcing. For example, as the lid is raised from 20 to 30 km, the resonant peak for $z_t=20$ km continuously shifts (illustrated by the arrows in Fig. 4) toward large vertical wavelength until it is replaced by another peak for $z_t=30$ km emerging from small vertical wavelength. The major peak for $z_t=20$ km is associated with the second vertical normal mode (M_2), while the major peak for $z_t=30$ km is associated with the third vertical normal mode (M_3). These normal modes have a different number (q) of nodes but have the same value of vertical scale (z_t/q).

It is also mentioned that if the forcing has more nodes ($q_0\gg1$) the envelope curve becomes sharper (not illustrated), since the projection coefficients become particularly large in the neighborhood of $M_q=M_0$.

In Fig. 4 the response curve was plotted as a function of the vertical wavenumber m which in turn varies with the frequency. If the response curve is plotted directly as a function of the frequency, the peak would look sharper when the frequency varies slowly with the vertical wavenumber than when the frequency varies rapidly, although the peak value does not change. The variation of the frequency with the vertical wavenumber is given by the dispersion relation (3.3) of gravity waves with (3.4) as

$$\omega\approx\pm\left(\frac{g\kappa}{H}\right)^{\frac{1}{2}}\frac{k}{|m|}, \tag{3.44}$$

$$-\frac{d\omega}{dm}\approx\pm\left(\frac{g\kappa}{H}\right)^{\frac{1}{2}}\frac{k}{m|m|}\approx\frac{\omega}{m}. \tag{3.45}$$

According to this relation $d\omega/dm$ at $m=M$ is proportional to k or ω. This means that in the neighborhood of the resonant peak at $m=M$, the frequency changes slowly if k or ω is small. Thus in the case of gravity waves the peak would look sharper for small k or ω.

Hereafter we shall refer to $-d\omega/dm$ as vertical group velocity, although it is not physically the speed of energy propagation that makes a frequency spectral peak sharp.

Our conclusion so far may be summarized as follows. A "non-singular resonance" associated with large finite amplitude occurs under the radiation condition, when the vertical scale of the wave coincides with that of the forcing confined in a lower layer. The frequency-spectral peak becomes sharp for waves associated with a small variation of frequency with vertical wavenumber. On the other hand, a singular resonance associated with infinitely large amplitude occurs under a lid condition, when a multiple of the vertical scale of the wave coincides with the height of the lid, a maximum response occurring for the vertical scale close to that of the forcing in the presence of dissipation. Although these conclusions are based on a gravity wave model in the absence of the Coriolis force, they are also valid in the presence of the Coriolis force except that the dispersion relation is different.

Our "non-singular resonance" is different from the frequency condensation point in wavenumber space discussed by Blandford (1966) and Munk and Phillips (1968) for ocean waves. In the case of the condensation point, the energy source has no distinct scale and the energy is concentrated at a frequency at which the group velocity becomes zero. In the case of our non-singular resonance under the radiation condition, the forcing has its own distinct vertical scale and the energy is concentrated at a frequency corresponding to the vertical scale of the forcing, as long as the change of frequency with vertical wavenumber is sufficiently small.

b. Equatorial wave model

Next we shall examine the resonance of equatorial waves on an equatorial beta plane.

1) ISOTHERMAL ATMOSPHERE

If we assume the heating of the form

$$J=2iJ_MP(y)\sin(Mz)e^{i(\omega t+kx)},\qquad J_M=0 \text{ for } z>z_1, \tag{3.46}$$

the solutions to (2.13)–(2.17) are given by

$$\begin{bmatrix}u\\v\\p\end{bmatrix}=-\begin{bmatrix}U(y)\\V(y)\\P(y)\end{bmatrix}\frac{\left[\left(im-\frac{1}{2H}\right)R_m^{1,2}e^{imz}\right]_{-m}^{m}-\left[\left(iM-\frac{1}{2H}\right)J_Me^{iMz}\right]_{-M}^{M}}{\frac{H}{\kappa}i\omega(m^2-M^2)}, \tag{3.47}$$

$$w=-P(y)\frac{\left[\left(im-\frac{1}{2H}+\frac{1}{h}\right)R_m^{1,2}e^{imz}\right]_{-m}^{m}-\left[\left(iM-\frac{1}{2H}+\frac{1}{h}\right)J_M e^{iMz}\right]_{-M}^{M}}{\frac{gH}{\kappa}(m^2-M^2)}, \tag{3.48}$$

where h is related to m of the homogeneous solution as

$$\left.\begin{aligned}\left(im-\frac{1}{2H}+\frac{1}{h}\right)\Big/\left(im-\frac{1}{2H}\right)\\ =-\frac{H}{\kappa}\left(im+\frac{1}{\gamma H}-\frac{1}{2H}\right)\end{aligned}\right\} \tag{3.49}$$

or equivalently

$$m^2=\frac{\kappa}{Hh}-\frac{1}{4H^2}$$

The horizontal structure functions satisfy the equatorial beta plane equations

$$\left.\begin{aligned}i\omega U(y)-\beta yV(y)+ikP(y)=0\\ \beta yU(y)+i\omega V(y)+\frac{dP(y)}{dy}=0\\ ikU(y)+\frac{dV(y)}{dy}+\frac{i\omega}{gh}P(y)=0\end{aligned}\right\}. \tag{3.50}$$

The eigensolutions of (3.50) with the boundary condition

$$U(y),\ V(y),\ P(y)\to 0 \quad \text{as} \quad y\to\pm\infty \tag{3.51}$$

are given by Matsuno (1966) and Lindzen and Matsuno (1968) as

$$V_n(y)=H_n(\epsilon^{\frac{1}{2}}y)\exp[-(\epsilon/2)y^2], \tag{3.52}$$

$$U_n(y)=-\frac{i(gh\epsilon)^{\frac{1}{2}}}{\omega}\left\{\frac{nH_{n-1}(\epsilon^{\frac{1}{2}}y)}{1-(k/\omega)(gh)^{\frac{1}{2}}}+\frac{\frac{1}{2}H_{n+1}(\epsilon^{\frac{1}{2}}y)}{1+(k/\omega)(gh)^{\frac{1}{2}}}\right\}\times\exp[-(\epsilon/2)y^2], \tag{3.53}$$

$$P_n(y)=\frac{igh\epsilon^{\frac{1}{2}}}{\omega}\left\{\frac{nH_{n-1}(\epsilon^{\frac{1}{2}}y)}{1-(k/\omega)(gh)^{\frac{1}{2}}}-\frac{\frac{1}{2}H_{n+1}(\epsilon^{\frac{1}{2}}y)}{1+(k/\omega)(gh)^{\frac{1}{2}}}\right\}\times\exp[-(\epsilon/2)y^2], \tag{3.54}$$

where $H_n(y)$ are Hermite's polynomial and

$$\epsilon\equiv\beta/(gh)^{\frac{1}{2}}. \tag{3.55}$$

The realistic heating function can be expanded horizontally by these eigenfunctions. Here we shall only examine a resonant response to a normal component of the heating. These eigenfunctions will be normalized by the latitudinal maximum value of $P(y)$ so that the latitudinal maximum of the heating (3.46) is given the same value for different n, ω, k and h.

The eigenvalue h is given by

$$(gh)^{\frac{1}{2}}=\frac{\beta(2n+1)}{2k^2[(\beta/k\omega)-1]}\times\left\{1\pm\left[1-\left(\frac{2\omega}{\beta}\right)^2\left(\frac{k}{2n+1}\right)^2\left(\frac{\beta}{k\omega}-1\right)\right]^{\frac{1}{2}}\right\},$$

$$\text{for } n=1, 2, 3, \ldots. \tag{3.56}$$

For mixed Rossby-gravity waves ($n=0$) and Kelvin wave ($n=-1$), h is given by

$$(gh_0)^{\frac{1}{2}}=\frac{\omega^2}{\beta-k\omega} \tag{3.57}$$

$$(gh_{-1})^{\frac{1}{2}}=\frac{\omega}{k}. \tag{3.58}$$

In order to include the effect of Newtonian cooling and Rayleigh friction, ω will be replaced by $\omega-i\alpha$ ($1/\alpha=15$ days) except for $e^{i\omega t}$. The vertical group velocities for $n=0$ and $n=-1$ are given by

$$-\frac{d\omega}{dm}=\left(\frac{H}{g\kappa}\right)^{\frac{1}{2}}\frac{m}{(m^2+\frac{1}{4}H^{-2})^{\frac{1}{2}}}\frac{\omega^3}{2\beta-k\omega}, \quad \text{for } n=0 \tag{3.59}$$

$$-\frac{d\omega}{dm}=-\left(\frac{g\kappa}{H}\right)^{\frac{1}{2}}\frac{m}{(m^2+\frac{1}{4}H^{-2})^{\frac{1}{2}}}\frac{k}{(m^2+\frac{1}{4}H^{-2})}, \quad \text{for } n=-1. \tag{3.60}$$

The frequency and the vertical group velocity of the equatorial normal modes are shown in Fig. 5 as a function of wavenumber for the observed vertical wavelength ($2\pi/m=10$ km). The vertical group velocity is small for low-frequency Rossby, mixed Rossby-gravity, and Kelvin waves, while it is large for high-frequency gravity waves.

The frequency and the vertical group velocity for wavenumber 4 as a function of vertical wavenumber is given in Fig. 6. It is seen that the frequency and the vertical group velocity decrease as vertical wavenumber increases.

From our previous discussion, small vertical scale equatorial waves with small vertical group velocity are expected to exhibit a sharp resonant peak even under the radiation condition, since the variation of their frequency with vertical wavenumber is small.

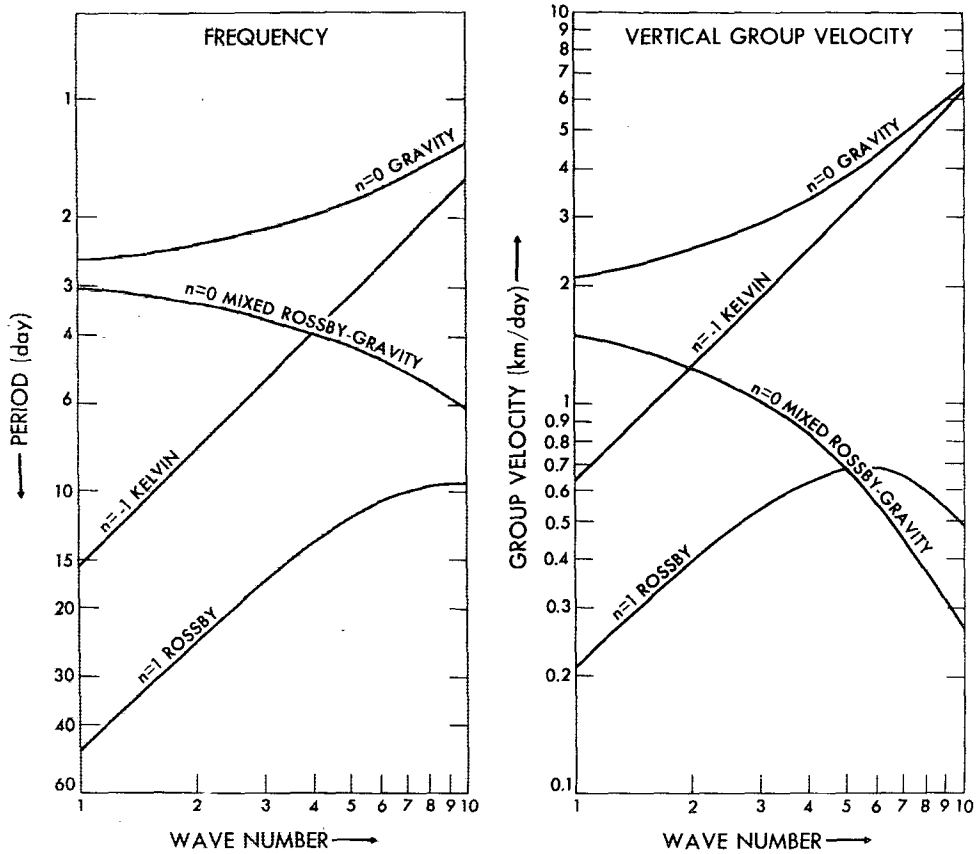

FIG. 5. Period and vertical group velocity of equatorial normal modes as a function of wavenumber for observed vertical wavelength ($2\pi/m=10$ km).

Fig. 7 shows the frequency response curve and the reflection coefficient of mixed Rossby-gravity wave ($n=0$) with wavenumber 4 for various heights of the lid. Two resonant peaks are seen. The major peak at a period of 3.3 days corresponds to the internal vertical mode with the vertical scale of the heating. The minor peak with a period of 2.3 days corresponds to external free oscillations, explained as follows.

The determinant of the algebraic equation for R_m is

$$|\mathbf{A}_m| \propto \begin{cases} \left(im-\frac{1}{2H}+\frac{1}{h}\right)e^{-imz_1}, & \text{for } R^2_{-m}=0 \quad (3.61) \\ \left(im-\frac{1}{2H}+\frac{1}{h}\right)\sin mz_t, & \text{for } w=0 \text{ at } z=z_t. \quad (3.62) \end{cases}$$

For both the upper boundary conditions, this determinant vanishes when

$$im-\frac{1}{2H}+\frac{1}{h}=0. \quad (3.63)$$

Such h is given by (3.63) and (3.49) as

$$h=\gamma H. \quad (3.64)$$

This corresponds to the eigenvalue of an external free oscillation in an isothermal atmosphere. If $h\neq\gamma H$ the algebraic equation has a solution which involves $1/[im-(2H)^{-1}+h^{-1}]$ in $R^{1,2}_{+m}$. As $h\to\gamma H$, $R^{1,2}_{+m}$ becomes infinite and u, v, p become infinite. However, w does not become infinite, since $R^{1,2}_{+m}$ is multiplied by $[im-(2H)^{-1}+h^{-1}]$ in (3.48). It is mentioned that w associated with the external free oscillation is identically zero. In Section 3a resonance for external waves has been ruled out by the approximation (3.5).

Fig. 7 also shows that the resonant peak of mixed Rossby-gravity waves under a lid placed at the 30 km level does not significantly change even if the lid is raised higher. Also the reflection coefficient (Fig. 7 right) is small. This assures that mixed Rossby-gravity waves simulated by a general circulation model are not spurious resonant waves resulting from an artificial reflection at the top of a finite-difference model.

Fig. 8 shows the resonant frequency and the resonant amplitude (kinetic energy at 15 km over the equator) of equatorial normal modes under the radiation condition as a function of wavenumber. In general, the lower the frequency, the larger the resonant response. This is because u and v (but not w) at $m=M$ increase with descreasing frequency as inferred

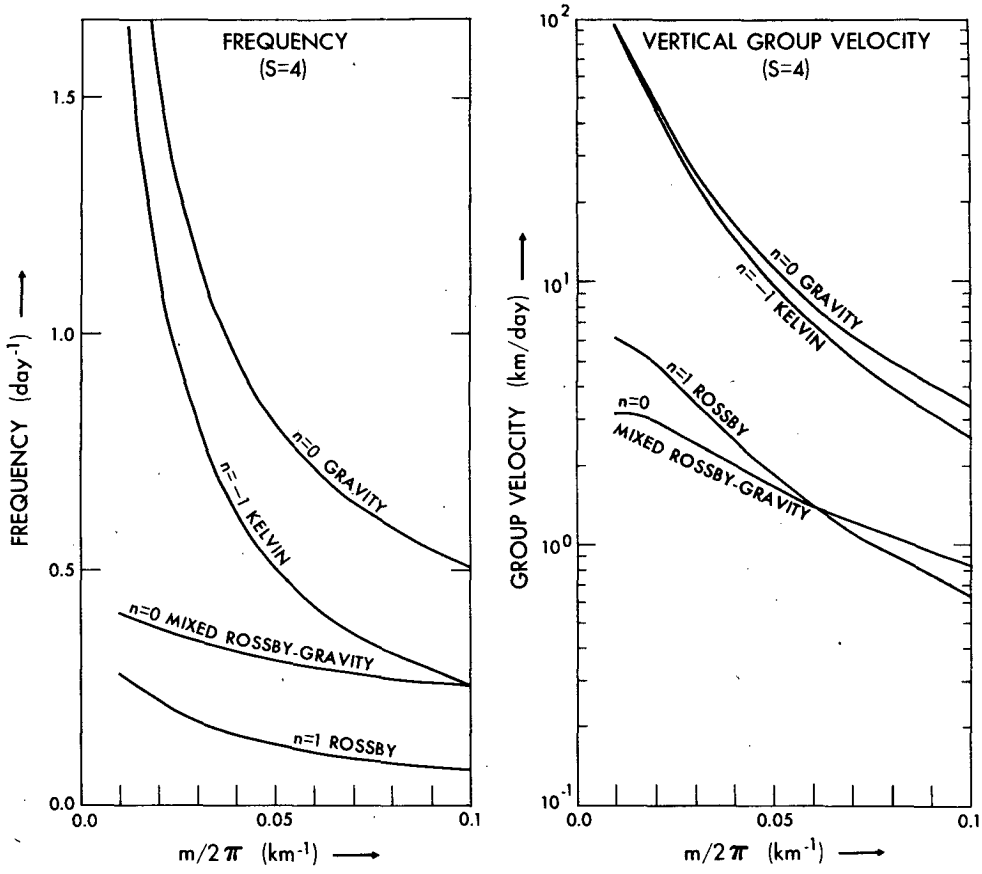

FIG. 6. Frequency and vertical group velocity of equatorial normal modes as a function of vertical wavenumber for wavenumber $s=4$.

from (3.47). Also, the lower the frequency, the sharper the frequency-spectral peak (not illustrated), since the vertical group velocity is smaller (see Fig. 5). It should be noted that Rossby wave ($n=1$) and Kelvin wave ($n=-1$) attain their maximum response at wavenumber 1. This feature agrees with the spectral analysis of the GFDL general circulation model (Hayashi, 1974). On the other hand, mixed Rossby-gravity waves ($n=0$) attain their maximum response at wavenumber 6 which is a little higher than the observed wavenumber 4. However, this preferred wavenumber and period decrease at higher levels (not illustrated). This feature is explained as follows. The amplitude decays with height above the level of the forcing due to the dissipation. Mixed Rossby-gravity waves with higher wavenumbers are associated with smaller vertical group velocity (see Fig. 5) and hence are attenuated more rapidly with height although their spectral peak is sharper. It is mentioned that in the absence of dissipation the resonant amplitude of mixed Rossby-gravity waves increases monotonically with wavenumber, since the frequency decreases.

2) REALISTIC VERTICAL DISTRIBUTION OF STATIC STABILITY AND HEATING

It is of interest to compare the resonant mixed Rossby-gravity waves with the observed Yanai-Maruyama waves or mixed Rossby-gravity waves simulated by a general circulation model. For this purpose we should use realistic vertical profiles of static stability and heating which affect the vertical wavenumber which in turn determines the resonant frequency.

The vertical structure equation in p-coordinates

$$\frac{d^2\omega(p)}{dp^2}+\frac{S_p}{gh}\omega(p)=-\frac{R}{ghC_pp}J(p) \qquad (3.65)$$

[where $\omega(p)$ is the vertical p-velocity], is solved numerically with a vertical resolution of 1 km up to 60 km level, using realistic stability (S_p) based on Hayashi (1970) and the U. S. Standard Atmosphere (1966) up to 60 km. The boundary condition is

$$\omega(p)=0 \quad \text{at } p=0 \text{ and } 1000 \text{ mb}. \qquad (3.66)$$

This upper boundary condition is equivalent to a free surface condition ($dp/dt=0$) and reflects energy at $p=0$ for a finite-depth fluid or a finite-difference model in the absence of dissipation. The vertical profile of heating is based on the GFDL general circulation model (see Hayashi, 1974).

Fig. 9 shows that the resonant period of mixed Rossby-gravity waves for wavenumber 4 is 3.3 days

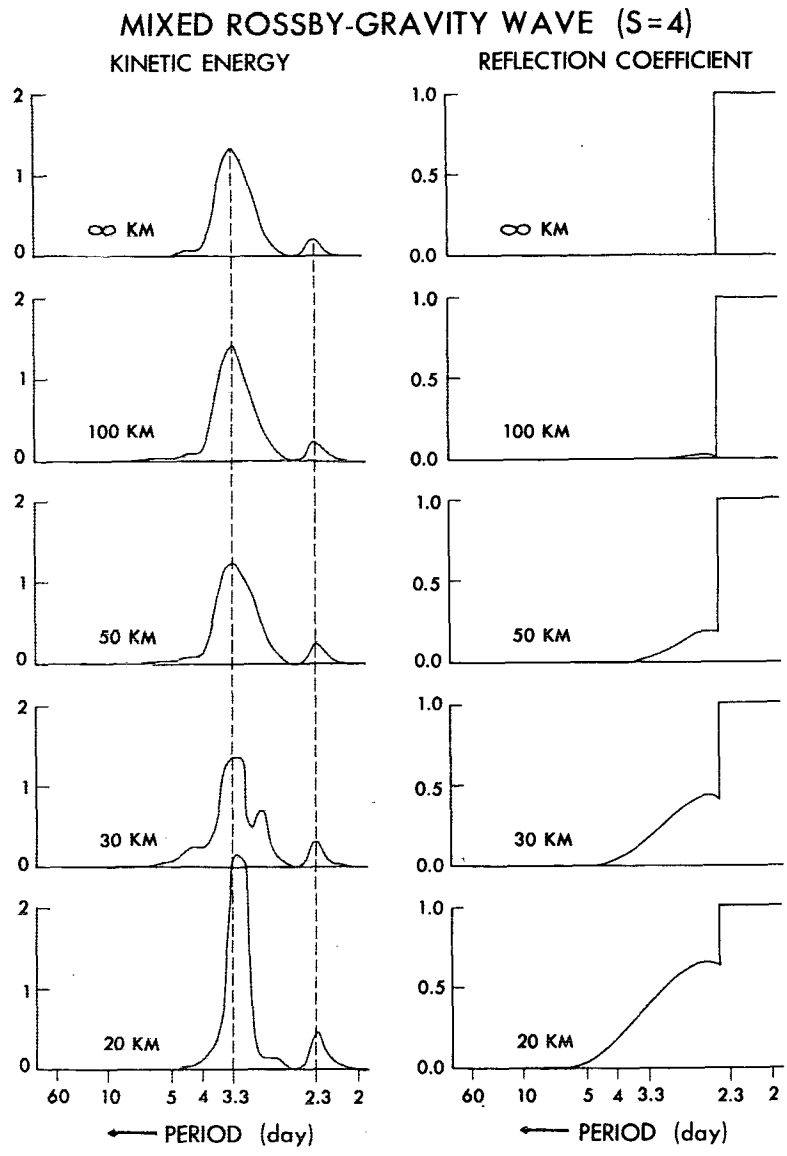

FIG. 7. Kinetic energy (left) of mixed Rossby-gravity waves ($n=0$, $s=4$) at $z=10$ km over the equator and reflection coefficient (right) as a function of period for various heights of lid. Reflection coefficient of external wave is defined as 1.0.

which is somewhat shorter than the observed 4–5 days or the eigenvalue (4 days) of a CISK model (Hayashi, 1970). The resonant peak for the external mode does not appear at a 2.3-day period because the lower boundary condition (3.66) is not valid for external waves.

Next we shall show that the vertical structure of the resonant mixed Rossby-gravity waves does not agree with observations. First it should be noted that the vertical structure of non-resonant mixed Rossby-gravity waves with the observed period of 4.6 days (Fig. 10a) looks similar to that of mixed Rossby-gravity waves (wavenumber 4, period 4.6 days) simulated by a GFDL general circulation model shown in Fig. 11. It is also similar to that of the observed Yanai-Maruyama waves (see Nitta, 1972) and the CISK waves (see Yamasaki, 1969; Hayashi, 1970). On the other hand, the vertical tilt of the resonant mixed Rossby-gravity waves with a period of 3.3 days (Fig. 10b) is smaller than that of the waves with the observed period. It is important to note that the heating and the vertical velocity in the troposphere are in quadrature for the resonant wave (Fig. 10b), while they are nearly in phase for the waves with the observed period (Fig. 10a).

The fact that the vertical velocity of internal waves and the heating are nearly in quadrature at resonance can be confirmed by the resonant solution in an isothermal atmosphere (3.25) since

$$w^1(z) \approx -i \frac{\kappa}{gHh} \frac{z_1^2}{2\pi} J_M \sin Mz, \quad \text{for} \quad 0<z<z_1. \tag{3.67}$$

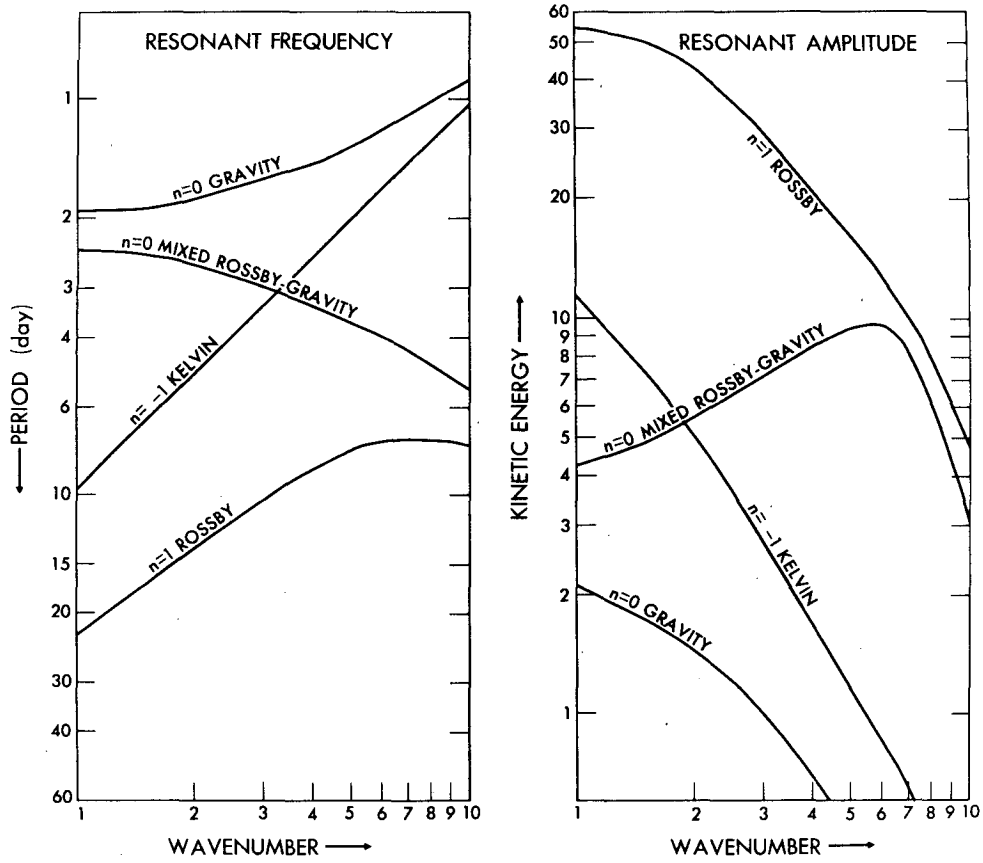

FIG. 8. Resonant frequency and resonant amplitude (kinetic energy at equator) of equatorial normal modes at $z=15$ km under the radiation condition as a function of zonal wavenumber ($\pi/m=10$ km, $1/\alpha=15$ days).

It is also inferred from (3.43), since

$$\lim_{m_r\to M}(m_r+im_i)^2-M^2\approx 2iMm_i, \tag{3.68}$$

and it is consistent with the balance of the available potential energy equation of the present model as

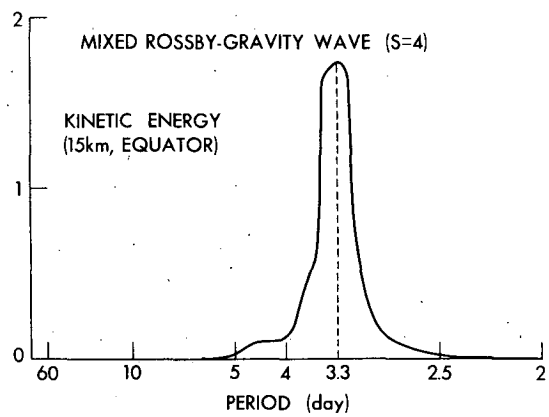

FIG. 9. Kinetic energy of mixed Rossby-gravity waves ($n=0$, $s=4$) at $z=15$ km over the equator for realistic vertical profile of static stability and heating.

given by

$$-\overline{\omega'\alpha'}=\frac{R}{S_pC_p\hat{p}}\overline{J'\alpha'}. \tag{3.69}$$

At resonance ω' becomes large for internal waves, while J' is fixed. In order for the left-hand and right-hand terms to balance, J' and α' should be nearly in phase with each other, while ω' and α' should be nearly in quadrature. If follows that J' and α' are in quadrature with ω'. It should be remembered that this phase relationship holds only for an equatorial normal mode component and not for an arbitrary meridional profile of heating which consists of several normal modes associated with different resonant frequencies. It does not hold for resonant external waves [Eq. (3.64)], since their vertical velocity does not become large even at resonance.

One may wonder whether such a phase relationship is consistent with the thermodynamic equation

$$\frac{\partial\alpha'}{\partial t}-S_p\omega'=\frac{R}{C_p\hat{p}}J', \tag{3.70}$$

even if $\partial\alpha'/\partial t$ and ω' are both in quadrature with J'.

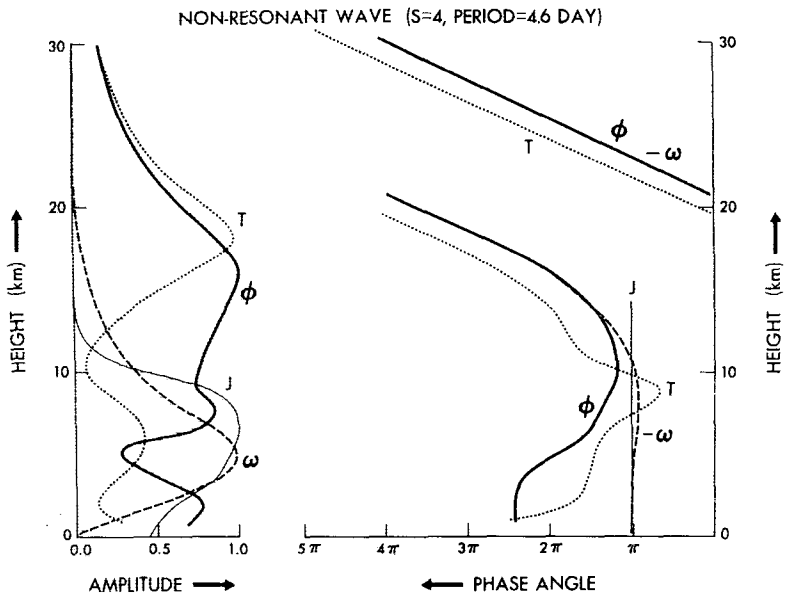

FIG. 10a. Vertical profile of amplitude and phase angle of non-resonant mixed Rossby-gravity waves (wavenumber 4, period 4.6 days). J=heating, ω=vertical, p-velocity, ϕ=geopotential, T=temperature, $1/\alpha=15$ days.

However, at resonance $\partial\alpha'/\partial t$ and ω' cancel each other to be in phase with J'. For the waves with the observed period, $\partial\alpha'/\partial t$ is small and $S_p\omega'$ almost balances with J'. In the lower troposphere (see Fig. 10a) J' and $-\omega'$ are in phase, and J' and α' are in quadrature, while in the upper troposphere J' and $-\omega'$ are not perfectly in phase and J' and α' become in phase.

In conclusion, this section has proven that although the resonance of equatorial waves to tropospheric thermal forcing is not suppressed by the radiation condition, the vertical structure does not agree with observations. The implications of this conclusion will be discussed in Section 5.

4. Lateral forcing

In this section we shall examine the resonance associated with mid-latitude forcing by imposing the radiation condition.

a. Gravity wave model

For the sake of simplicity we shall neglect the Coriolis parameter and prove that the resonance to

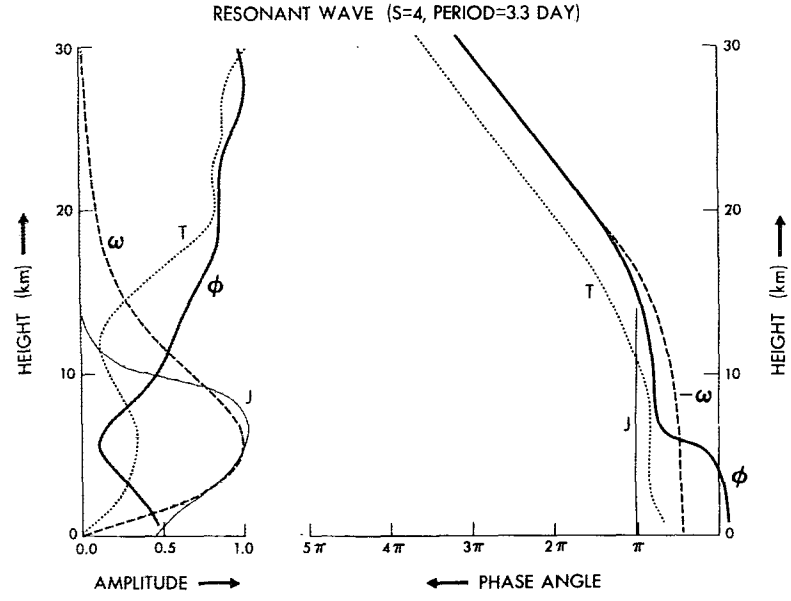

FIG. 10b. As in Fig. 10a except for resonant waves (period 3.3 days).

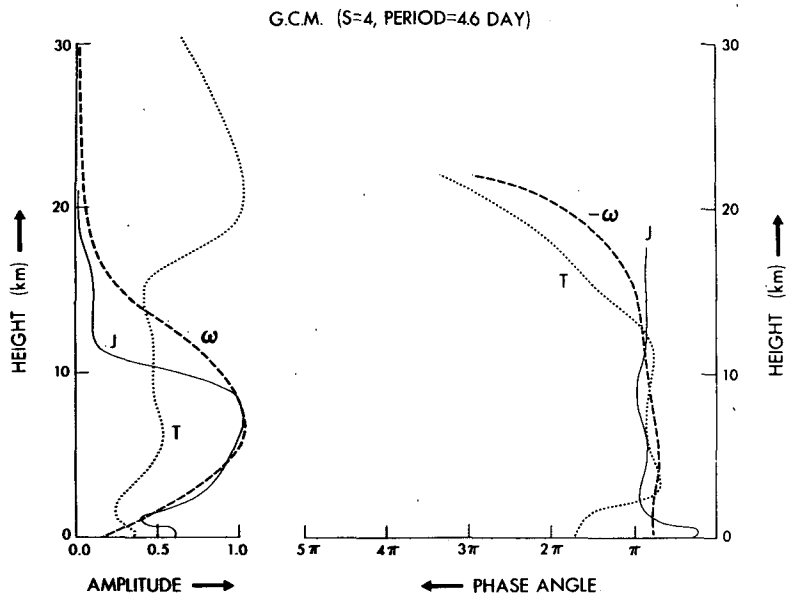

FIG. 11. Vertical profile of amplitude and phase difference of mixed Rossby-gravity waves (wavenumber 4, period 4.6 days, westward moving) at 14.4°N simulated by GFDL general circulation model during the period April through September. J = diabatic heating (convective heating and sensible heat from the surface).

the lateral forcing is associated with finite amplitude under the radiation condition.

The lateral forcing at $y=\pm y_b$ is assumed to be symmetric with respect to the equator and propagating vertically as

$$v=Re^{i(Mz+kx+\omega t)}. \tag{4.1}$$

The lower boundary condition is

$$w=0 \quad \text{at} \quad z=0. \tag{4.2}$$

The complete solutions of (2.13)–(2.17) for $J=0, f=0$ satisfying the radiation condition are given by

$$v=-\left(\sum_{n=1}^{\infty} v_n-v_0\right)/\cos l_0 y_b, \tag{4.3}$$

$$w=-\left(\sum_{n=1}^{\infty} w_n-w_0\right)/\cos l_0 y_b, \tag{4.4}$$

where

$$v_n=R_n\cos(l_n y)e^{i(m_n z+kx+\omega t)}, \tag{4.5}$$

$$w_n=-\frac{\omega^2 H}{g\kappa}R_n\frac{\sin l_n y}{l_n}(im_n+\mu)e^{i(m_n z+kx+\omega t)}, \tag{4.6}$$

$$\text{for} \quad n=0,1,2\ldots,$$

$$\mu\equiv\frac{1}{\gamma H}-\frac{1}{2H}. \tag{4.7}$$

In (4.6) the following relation given by (3.49) has been used:

$$im_n+\mu=-\frac{\kappa}{H}\left(im_n-\frac{1}{2H}+\frac{1}{h_n}\right)\Big/\left(im_n-\frac{1}{2H}\right). \tag{4.8}$$

In the above solutions, v_0 matches with the lateral forcing at $y=\pm y_b$ as

$$R_0=R, \quad m_0=M. \tag{4.9}$$

The dispersion relation gives l_0 as

$$l_0^2=\frac{H}{g\kappa}\omega^2\left(M^2+\frac{1}{4H^2}\right)-k^2. \tag{4.10}$$

On the other hand, v_n $(n\geqslant 1)$ are normal mode solutions in the horizontal as

$$v_n=0 \quad \text{at} \quad y=\pm y_b. \tag{4.11}$$

The lower boundary condition is satisfied by w_0 together with w_n $(n\geqslant 1)$ as

$$\sum_{n=1}^{\infty} w_n-w_0=0 \quad \text{at} \quad z=0. \tag{4.12}$$

It is mentioned that these normal mode solutions $(n\geqslant 1)$ do not appear in the analytical solution of Lamb (1973) who did not impose the radiation condition rigorously. From (4.11) we have

$$l_n=\frac{\pi}{2}\frac{2n-1}{y_b}. \tag{4.13}$$

The dispersion relation gives m_n as

$$m_n^2=\frac{g\kappa}{H}\frac{l_n^2+k^2}{\omega^2}-\frac{1}{4H^2}. \tag{4.14}$$

From (4.12) we have

$$\sum_{n=1}^{\infty} R_n\frac{\sin l_n y}{l_n}(im_n+\mu)=R_0\frac{\sin l_0 y}{l_0}(im_0+\mu). \tag{4.15}$$

Inverting (4.15), R_n is given explicitly as

$$R_n=R_0\frac{im_0+\mu}{im_n+\mu}\frac{2l_n}{l_n+l_0}\frac{\sin(l_n-l_0)y_b}{(l_n-l_0)y_b}. \tag{4.16}$$

Rewriting (4.10) by combining with (4.14), we have

$$l_0^2-l_n^2=-\frac{H}{g\kappa}\omega^2(m_n^2-M^2). \tag{4.17}$$

From (4.17) we see that

If $m_r(k,\omega)=M$, then $l_0=l_r$ and $\cos l_0 y_b=0$. (4.18)

This means that if k and ω of the forcing are such that the vertical wavenumber (m_r) of one of the normal mode solutions (v_n) matches the vertical wavenumber (M) of the forcing, the denominator of v vanishes.

On the other hand, (4.16) gives

$$\text{If } m_r(\omega,k)=M, \text{ then}$$
$$R_n=\begin{cases}R_0, & \text{for } n=r\\ 0, & \text{for } n\neq r\end{cases} \tag{4.19}$$

Therefore

$$\sum_{n=1}^{\infty} v_n-v_0=0 \quad \text{for} \quad m_r(\omega,k)=M. \tag{4.20}$$

This proves that the resonance[6] to the lateral forcing propagating vertically is associated with finite amplitude under the radiation condition. The sharpness of the frequency-spectral peak depends on $d\omega/dm$. For a forcing confined in a lower layer, the solution in the lower layer consists of both upward and downward propagating waves and is matched with an upward propagating wave in the upper layer. It may similarly be proven that a non-singular resonance occurs when the vertical scale of the wave in the upper layer coincides with that of the lateral forcing in the lower layer.

[6] This resonant solution may be obtained either by L'Hôpital's rule or directly from (2.13)–(2.17) by assuming the solution of the form

$$v=A(y\sin l_0 y)e^{iMz}+B\cos l_0 y(ze^{iMz})+\sum_{n=1}^{\infty}C_n\cos l_n y e^{iM_n z}.$$

b. Equatorial wave model

Now we shall examine the resonance of tropical waves to mid-latitude forcing under the radiation condition on an equatorial beta-plane. It is easier to use the vertical expansion method to solve this problem than the vertical matching method.

The middle latitude forcing at $y=\pm y_b$ is assumed to be

$$v=\begin{cases}R\cos(M_0 z)e^{i(kx+\omega t)}, & \text{for } 0\leqslant z\leqslant z_1\\ 0, & \text{for } z_1<z\leqslant z_t\end{cases}, \tag{4.21}$$

where

$$M_0=\pi q_0/z_1. \tag{4.22}$$

This forcing is expanded in terms of the vertical normal modes. The complete solutions of (2.13)–(2.17) under a lid condition for $J=0$ are given by

$$\begin{bmatrix}u\\ v\\ p\end{bmatrix}=\sum_{q=1}^{\infty}\frac{R_q}{V_q(y_b)}\begin{bmatrix}U_q(y)\\ V_q(y)\\ P_q(y)\end{bmatrix}\cos(M_q z)e^{i(kx+\omega t)}, \tag{4.23}$$

$$w=\frac{i\omega H}{g\kappa}\sum_{q=1}^{\infty}\frac{R_q}{V_q(y_b)}P_q(y)M_q\sin(M_q z)e^{i(kx+\omega t)}, \tag{4.24}$$

where

$$M_q=\frac{q\pi}{z_t}, \tag{4.25}$$

$$R_q=\frac{2\delta q}{q+q_0/\delta}\frac{\sin\pi(\delta q-q_0)}{\pi(\delta q-q_0)}, \tag{4.26}$$

$$\delta=z_1/z_t. \tag{4.27}$$

In (4.24) the following relation for a homogeneous solution has been used:

$$\left(iM_q-\frac{1}{2H}+\frac{1}{h_q}\right)\Big/\left(iM_q-\frac{1}{2H}\right)$$
$$=-\frac{H}{\kappa}\left(iM_q+\frac{1}{\gamma H}-\frac{1}{2H}\right)\approx\frac{H}{\kappa}iM_q. \tag{4.28}$$

The approximation in (4.28) does not hold for small M_q but the projection coefficient R_q is small when M_q is small. In the above, the horizontal structure functions are as follows (see Koss, 1967):

$$V_q(y)=\exp[-(\epsilon_q/2)y^2]M^1, \tag{4.29}$$

$$P_q(y)=\frac{(gh_q)^{\frac{1}{2}}}{ik[\omega/k+(gh_q)^{\frac{1}{2}}]}\beta y\exp[-(\epsilon_q/2)y^2]$$
$$\times\left[M^1-\frac{4a_q(\omega/k)}{\omega/k-(gh_q)^{\frac{1}{2}}}M^2\right], \tag{4.30}$$

$$U_q(y)=\frac{1}{ik[\omega/k+(gh_q)^{\frac{1}{2}}]}\beta y\exp[-(\epsilon_q/2)y^2]$$
$$\times\left[M^1+\frac{4a_q(\omega/k)}{\omega/k-(gh_q)^{\frac{1}{2}}}M^2\right], \quad (4.31)$$

where

$$\left.\begin{aligned}M^1&=M(a_q,\tfrac{1}{2},\epsilon_q y^2)\\ M^2&=M(a_q+1,\tfrac{3}{2},\epsilon_q y^2)\end{aligned}\right\} \quad (4.32)$$

which are the confluent hypergeometric functions and

$$h_q=\frac{\kappa}{H(M_q^2+\frac{1}{4}H^{-2})} \quad (4.33)$$

$$\epsilon_q=\frac{\beta}{(gh_q)^{\frac{1}{2}}} \quad (4.34)$$

$$4a_q=1-\left(\frac{\beta k}{\omega}-k^2+\frac{\omega^2}{gh_q}\right)\frac{(gh_q)^{\frac{1}{2}}}{\beta}. \quad (4.35)$$

If $-2a_q=n$ (integer) the above horizontal structure functions coincide with (3.52)–(3.54) as discussed by Rosenthal (1965). A singular resonance occurs when $a_q(\omega,k)$ is such that $V_q(y_b)$ vanishes. In order to avoid this singularity, we shall add small dissipation and replace ω by $\omega-i\alpha$ except for $e^{i\omega t}$. Then a_q and $V_q(y)$ become complex. Since $V_q(y)$ is complex, v in (4.23) changes its phase with height, although the single vertical normal mode component of v does not change its phase since M_q is real.

Let us compare our model with the analytical model of Lamb (1973). Instead of imposing an upper boundary condition, Lamb (1973) assumed that the vertical structure of the forced wave is everywhere the same as that of the forcing characterized by a complex vertical wavenumber (M) which gives a net upward flux of energy as follows.

The vertical structure of her solution is given by a single vertical wavenumber as

$$w=2i\sin Mz$$
$$=e^{iM_r z}e^{-iM_i z}-e^{-iM_r z}e^{M_i z}, \quad \text{for } 0\leq z\leq z_1. \quad (4.36)$$

If $M_i<0$, the first term dominates the second, giving net upward flux of energy. However, there is no guarantee that the energy leaking from $z=z_1$ will not further be reflected from above, since the solution (4.36) which amplifies indefinitely with height is not valid above $z=z_1$.

In our problem we shall place the lid as high as 100 km to simulate the radiation condition. The forcing is assumed to be white noise and has the vertical wavelength ($2\pi/M$) of 10 km, vanishing above 10 km. The lateral boundary is placed at 24° latitude. This model is similar to the finite-difference model of Lamb (1973).

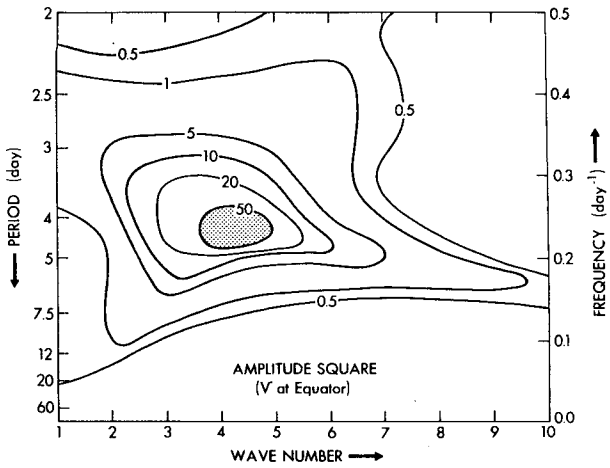

FIG. 12a. Amplitude square of meridional component of wind at $z=5$ km over the equator as a function of wavenumber and period (westward moving).

Fig. 12a shows that a maximum response of the v component at the equator occurs at wavenumber 4 and a period of 4 days. This result is not altered even if the lid is raised higher (not illustrated). This confirms that even under the radiation condition, the resonant peak found by Mak (1969) and Lamb (1973) still remain as a significant spectral peak.

However, Fig. 12b shows that a resonant peak occurs even at the lateral boundary for p as a feedback to the imposed meridional component which is assumed to have no spectral peak. The zonal component shows a response curve similar to Fig. 12b (not illustrated).

Moreover, Fig. 13 shows that u and p of the most resonant wave increases toward the lateral boundary, while v decays away from the equator. Also the phase line of p tilts in such a way as to be in phase or 180° out of phase with v at the boundary. This phase relation occurs along the maximum response line in Fig. 12b. Thus the large meridional flux of energy

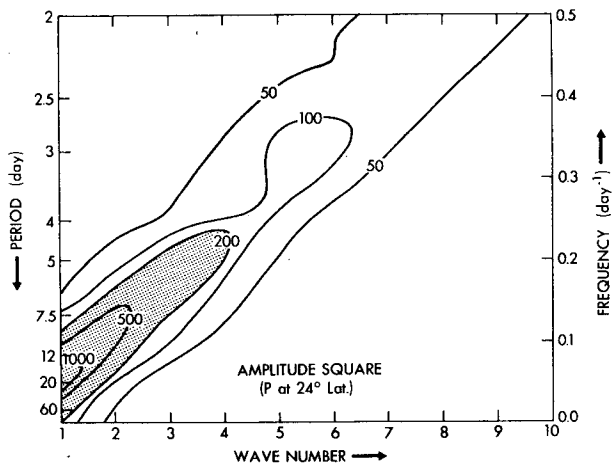

FIG. 12b. As in Fig. 12a except for pressure at 24° latitude.

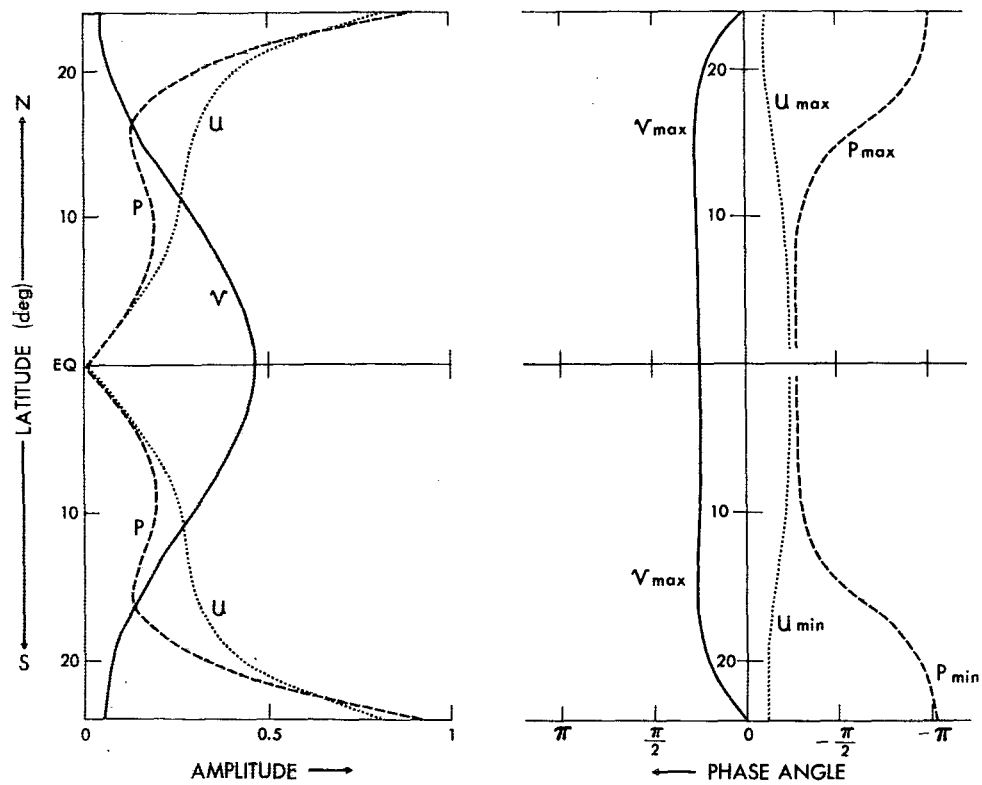

FIG. 13. Latitudinal profiles of amplitude and phase angle of resonant equatorial wave with wavenumber 4 and period of 4.3 days at 5 km level.

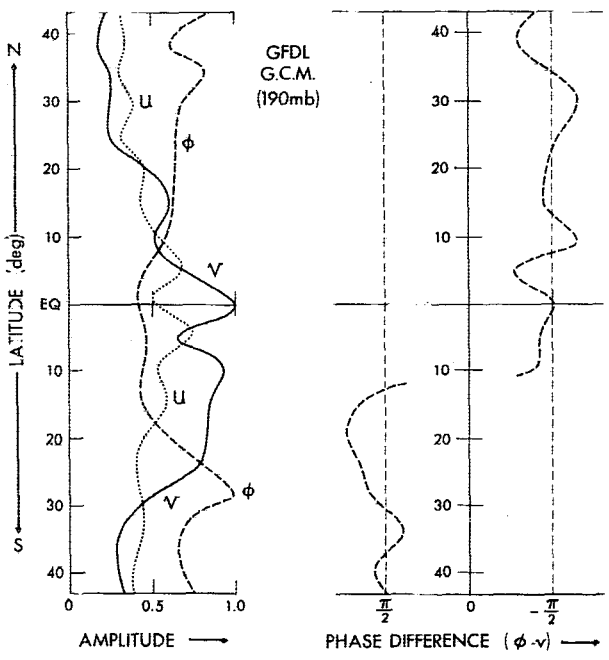

FIG. 14. Latitudinal profiles of amplitude and phase difference between ϕ and v of disturbances (wavenumber 4; period 4.6 days, westward moving) at 190 mb simulated by GFDL general circulation model during the period April through September.

associated with the resonant wave is due to this phase relation as well as the large amplitude of p. It is mentioned that the pressure is not in geostrophic balance with the meridional component of the mid-latitude forcing.

This resonant wave corresponds to the $n=0$ "invalid" normal mode on an equatorial beta plane with westward phase velocity $[\omega/k=(gh)^{\frac{1}{2}}]$ rather than to the $n=0$ mixed Rossby-gravity waves. This mode is not accepted as a normal mode over a sphere, since u and p do not decay with latitude as pointed out by Matsuno (1966). However, it is a legitimate normal mode[7] of a tropical channel model and appears in the dispersion relation curve of Mak (1969).

It will be of interest to see whether these characteristics of the resonant equatorial waves are seen in a general circulation model. Fig. 14 shows the horizontal structure of disturbances with wavenumber 4 and period of 4.6 days moving westward at 190 mb in the GFDL general circulation model. At higher levels than 190 mb these disturbances take the form of normal mode mixed Rossby-gravity waves (see Hayashi, 1974). In contrast to the resonant equatorial waves, the u component in Fig. 14 does not increase with latitude, although it increases with

[7] This mode may be interpreted as a westward-moving antisymmetric Kelvin wave coasting along the boundaries away from the equator (see Lindzen, 1970).

latitude for long-period oscillations (not illustrated). The reason why Mak (1969) found agreement with observation may be that he compared the variance of the u component which is dominated by long-period oscillations. Fig. 14 also shows that the geopotential height is nearly in quadrature with the v component throughout the latitudes. Furthermore, the geopotential height and the meridional flux of energy do not exhibit such sharp spectra with westward phase velocity in the middle latitudes (not illustrated) as expected from the resonant theory.

5. Conclusions and remarks

Based on an equatorial beta-plane model without wind shear, the following conclusions have been made concerning the response of equatorial internal waves to a thermal or a lateral forcing confined in the troposphere:

1) A "non-singular resonance" associated with large finite amplitude occurs under the radiation condition, when the vertical scale of the wave in a free isothermal atmosphere coincides with that of the forcing. On the other hand, a "singular resonance" associated with infinite amplitude occurs under a lid condition, when a multiple of the vertical scale of the wave coincides with the height of the lid, a maximum response occurring in the presence of dissipation for the vertical scale of the wave close to that of the forcing.

2) A frequency spectral peak due to a non-singular resonance is sharp for waves associated with a small change of frequency with vertical wavenumber such as equatorial waves with small vertical scale.

3) The resonant period of thermally forced mixed Rossby-gravity waves for wavenumber 4 is 3.3 days and the vertical wavelength in the stratosphere is about 15 km whereas the observed period and vertical wavelength are $\sim$4–5 days and $\sim$5–10 km, respectively.

4) The heating and the temperature are nearly in quadrature with the vertical velocity associated with the resonant internal equatorial-normal mode contrary to observations, while they are in phase with the vertical velocity of non-resonant mixed Rossby-gravity waves with period of 4.6 days.

5) A maximum resonant response to symmetric lateral forcing occurs at wavenumber 4 and 4-day period, if the vertical wavelength of the forcing is 10 km.

6) This resonant wave is characterized by the increase of pressure and zonal component with latitude. At the lateral boundary the pressure exhibits a sharp resonant peak for westward phase velocity and is in phase or 180° out of phase with the meridional component contrary to the general circulation model.

7) The equatorial waves simulated by a general circulation model are not spurious resonant waves artificially reflected by the top of the finite-difference model and will not disappear even if the radiation condition is imposed.

Based upon the present results it is difficult to interpret the observed Yanai-Maruyama waves as resonant waves. The reason why such a resonance does not occur in the tropical atmosphere may be that the resonant waves do not conform to some constraint between the forcing and its feedback. In the case of the CISK theory, for example, the heating is parameterized in such a way that the convective heating is in phase with the vertical velocity at the top of the boundary layer. This is why the eigenfrequency of a CISK model does not coincide with the resonant frequency of a dry atmosphere. In the case of a general circulation model with the moist convective adjustment, the convective heating is also implicitly related to the vertical velocity through the horizontal convergence of moisture. In the case of mid-latitude forcing, it is required dynamically that the pressure of equatorial waves be continuous with that of mid-latitude disturbances across the latitude where the meridional component of the mid-latitude disturbances is imposed. It is likely that the forcing is not associated with a component having such frequency, vertical and horizontal scale as to cause resonance.

In this model the meridional structure of the heating was assumed to take the form of an equatorial normal mode. Therefore the meridional structure of the vertical velocity necessarily takes the same form as that of the heating for all wavenumbers and frequencies. Furthermore the meridional expanse of the equatorial normal mode also varies slowly with the equivalent depth which in turn varies with wavenumber and frequency. It is of importance to re-examine the resonant response and the relations between the imposed heating and the vertical velocity by a model with realistic horizontal distribution of heating and wind shear.

Acknowledgments. The author wishes to express his hearty thanks to Drs. I. Orlanski, S. B. Fels, S. Manabe and K. Miyakoda for their valuable comments and suggestions, and to Mr. D. G. Golder for reading the manuscript. He is also grateful to Dr. J. Smagorinsky for his interest and encouragement. Thanks are extended to Mr. P. Tunison for drafting, Mr. J. N. Conner for photographing, and Mrs. C. A. Longmuir for typing.

APPENDIX

List of Symbols

x,y,z	zonal, meridional and vertical coordinates
u,v,w	eastward, northward and vertical velocity
p	pressure
ρ	density

J external heat excitation per unit mass per unit time
g acceleration by gravity
R gas constant
C_p specific heat at constant pressure
C_v specific heat at constant volume
γ C_p/C_v $(=1.4)$
κ $(\gamma-1)/\gamma$
f Coriolis parameter
H scale height

REFERENCES

Bennett, J. R., and J. A. Young, 1971: The influence of latitudinal wind shear upon large-scale wave propagation into the tropics. *Mon. Wea. Rev.*, **99**, 202–214.

Blandford, R., 1966: Mixed gravity–Rossby waves in the ocean. *Deep-Sea Res.*, **13**, 941–961.

Charney, G., 1969: A further note on large-scale motions in the tropics. *J. Atmos. Sci.*, **26**, 182–185.

Gruber, A., 1974: The wavenumber-frequency spectra of satellite measured brightness in the tropics. *J. Atmos. Sci.*, **31**, 1675–1680.

Hayashi, Y., 1970: A theory of large-scale equatorial waves generated by condensation heat and accelerating the zonal wind. *J. Meteor. Soc. Japan*, **48**, 140–160.

——, 1971a: Instability of large-scale equatorial waves under the radiation condition. *J. Meteor. Soc. Japan*, **49**, 315–318.

——, 1971b: Large-scale equatorial waves destabilized by convective heating in the presence of surface friction. *J. Meteor. Soc. Japan*, **49**, 458–466.

——, 1971c: Instability of large-scale equatorial waves with a frequency-dependent CISK parameter. *J. Meteor. Soc. Japan*, **49**, 59–62.

——, 1973: A method of analyzing transient waves by space-time cross spectra. *J. Appl. Meteor.*, **12**, 404–408.

——, 1974: Spectral analysis of tropical disturbances appearing in a GFDL general circulation model. *J. Atmos. Sci.*, **31**, 180–218.

Holton, J. R., 1972: Waves in the equatorial stratosphere generated by tropospheric heat sources. *J. Atmos. Sci.*, **29**, 368–375.

——, 1973: On the frequency distribution of atmospheric Kelvin waves. *J. Atmos. Sci.*, **30**, 499–501.

——, and R. S. Lindzen, 1968: A note on Kelvin waves in the atmosphere. *Mon. Wea. Rev.*, **96**, 385–396.

Koss, W. J., 1967: Further theoretical considerations of tropical wave motions in the equatorial latitudes. *Mon. Wea. Rev.*, **95**, 283–297.

Kuo, H.-L., 1975: Instability theory of large-scale disturbances in the tropics. *J. Atmos. Sci.*, **33**, 2229–2245.

Lamb, V. R., 1973: The response of a tropical atmosphere to middle latitude forcing. Ph.D. thesis, University of California, Los Angeles.

Lindzen, R. S., 1967: Planetary waves on beta planes. *Mon. Wea. Rev.*, **95**, 441–451.

——, 1970. Internal equatorial planetary-scale waves in shear flow. *J. Atmos. Sci.*, **27**, 394–407.

——, and R. Matsuno, 1968: On the nature of a large-scale wave disturbances in the equatorial lower stratosphere. *J. Meteor. Soc. Jap.*, **46**, 215–221.

——, E. S. Batten and J. W. Kim, 1968: Oscillations in atmosphere with tops. *Mon. Wea. Rev.*, **96**, 133–140.

Longuet-Higgins, M. S., 1968: The eigenfunctions of Laplace's tidal equations over a sphere. *Phil. Trans. Roy. Soc. London*, **A262**, 511–607.

Mak, M. K., 1969: Laterally driven stochastic motions in the tropics. *J. Atmos. Sci.*, **26**, 41–64.

Manabe, S., J. L. Holloway, Jr., and H. M. Stone, 1970: Tropical circulation in a time integration of a global model of the atmosphere. *J. Atmos. Sci.*, **27**, 580–613.

Maruyama, T., 1967: Large-scale disturbances in the equatorial lower stratosphere. *J. Meteor. Soc. Japan*, **45**, 391–408.

Matsuno, T., 1966: Quasi-geostrophic motions in the equatorial area. *J. Meteor. Soc. Japan*, **44**, 25–43.

Munk, W., and N. Phillips, 1968: Coherence and band structure of inertial motion in the sea. *Rev. Geophys.*, **6**, 447–472.

Nitta, Tsuyoshi, 1972: Structure of wave disturbances over the Marshall Islands during the years of 1956 and 1958. *J. Meteor. Soc. Japan*, **50**, 85–103.

Orlanski, I., 1972: On the breaking of standing internal gravity waves. *J. Fluid Mech.*, **54**, 577–598.

Rosenthal, S. L., 1965: Some preliminary theoretical considerations of tropospheric wave motions in equatorial latitudes. *Mon. Wea. Rev.*, **93**, 605–612.

Sommerfeld, A., 1949: *Partial Differential Equations in Physics.* Academic Press, 329 pp.

Wallace, J. M., and V. E. Kousky, 1968: Observational evidence of Kelvin waves in the tropical stratosphere. *J. Atmos. Sci.*, **25**, 900–907.

Wilkes, M. V., 1949: *Oscillations of the Earth's Atmosphere.* Cambridge University Press, 76 pp.

Yamasaki, M., 1969: Large-scale disturbances in a conditionally unstable atmosphere in low latitudes. *Pap. Meteor. Geophys.*, **20**, 289–336.

Yanai, M., and T. Maruyama, 1966: Stratospheric wave disturbances propagating over the equatorial Pacific. *J. Meteor. Soc. Japan*, **44**, 291–294.